

# Hydrogenated Ring-Opened Poly(*endo*-dicyclopentadiene)s Made via Stereoselective ROMP Catalyzed by Tungsten Complexes: Crystalline Tactic Polymers and Amorphous Atactic Polymer

Shigetaka Hayano, Yoshihisa Takeyama, Yasuo Tsunogae,\* and Ichiro Igarashi

Zeon Corporation, 1-2-1 Yako, Kawasaki-ku, Kawasaki, 210-9507, Japan

Received February 28, 2006; Revised Manuscript Received April 19, 2006

**ABSTRACT:** Properties of the tactic and atactic hydrogenated ring-opened poly(*endo*-dicyclopentadiene)s and features of the tungsten imido/phenolate-catalyzed stereoselective ring-opening metathesis polymerizations (ROMP) were studied. Several tungsten(VI) imido phenolate complexes were synthesized and exhibited moderate ROMP activity in the presence of *n*-BuLi. W(=NPh)((*R*)-(+)-5,5',6,6'-Me<sub>4</sub>-3,3'-*t*-Bu<sub>2</sub>-biphenolate)<sub>2</sub> was found to be effective for *cis*-, isoselective ROMP of *endo*-dicyclopentadiene (DCPD), while W(=NPh)Cl<sub>4</sub>·Et<sub>2</sub>O promoted *cis*-, syndiospecific ROMP. On the other hand, W(=NPh)(2,6-Me<sub>2</sub>-phenolate)<sub>4</sub> provided atactic poly(DCPD). Isotactic, atactic, and syndiotactic hydrogenated ring-opened poly(DCPD)s were characterized well by various methods for the first time. Both tactic polymers were shown to be crystalline polymers by means of DSC, WAXD, and TEM measurements. In contrast, atactic poly(DCPD) was an amorphous polymer. The crystallization rate of the syndiotactic hydrogenated poly(DCPD) was significantly higher than that of the isotactic polymer.

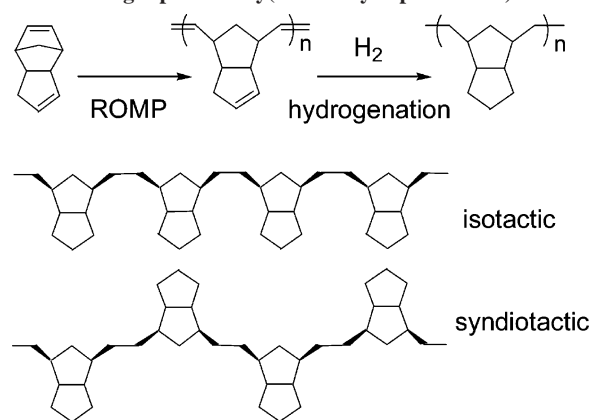
## Introduction

Cycloolefins are recognized as versatile monomers, which easily polymerize in the presence of metathesis catalysts to form ring-opened poly(cycloolefin)s. It is well-known that the development of well-defined catalysts, metal carbene complexes, and some non-carbene complexes has paved the way to the precise ring-opening metathesis polymerization (ROMP) of cycloolefins.<sup>1</sup> To the best of our knowledge, most of the precise ROMP systems were achieved by the well-defined carbene complexes such as the Schrock catalysts and the Grubbs catalysts.<sup>2,3</sup> The stereospecific ROMP of cycloolefins has been studied in detail for many years.<sup>4</sup> In the case of ring-opened poly(cycloolefin), there are three different steric structural factors (head–head/head–tail/tail–tail, *cis/trans*, meso/racemo) which define the polymer backbone.

*endo*-Dicyclopentadiene (DCPD), a tricyclic olefin, is also a versatile monomer and one of the main distillates of crude petroleum. It can be polymerized by various metathesis catalysts to high molecular weight, by opening the strained norbornene ring and retention of the less-strained cyclopentene ring (Scheme 1). The *cis/trans* configuration of the double bond in the main chain has a unique effect on the properties of the ring-opened poly(DCPD). However, the unsaturated nature of poly(DCPD) makes it susceptible to oxidative degradation. This problem could be solved by hydrogenation of the double bonds. The characterization and properties of hydrogenated ring-opened poly(cycloolefin)s have been under intensive research.<sup>5,6</sup> The properties of hydrogenated ring-opened poly(cycloolefin)s are generally very different from those of the unsaturated poly(cycloolefin)s. The properties of hydrogenated atactic polynorbornene and block copolymers containing hydrogenated polynorbornene sequence were investigated in full by Register et al.<sup>7</sup> We have studied hydrogenated poly(DCPD)s and hydrogenated tactic polynorbornene briefly.<sup>8</sup>

Recently, we have reported that the molybdenum-based catalysts bearing substituted diolate ligands, MoO(*R*)-(+)–

**Scheme 1. Synthesis and Structures of Hydrogenated Ring-Opened Poly(*endo*-Dicyclopentadiene)**



5,5',6,6'-Me<sub>4</sub>-3,3'-*t*-Bu<sub>2</sub>-biphenolate)<sub>2</sub>, promoted *cis*-, isoselective ROMP of DCPD and norbornene.<sup>8a,b</sup> More recently, *cis*-, syndiospecific ROMP of DCPD was accomplished using tungsten imido-based catalysts.<sup>8c,d</sup> However, the effects of imido and phenolate ligands on the tacticity control were not studied fully enough in these two ROMP systems. Therefore, it appeared interesting to investigate how the polymerization process would be regulated by the combination of imido and phenolate ligands. Also, the crystal nature of the isotactic and syndiotactic poly(DCPD)s seemed to be insufficiently well studied. Particularly, the relationship between stereostructure and property of these polymers has not yet been clarified.

For these reasons, we have studied these new stereoselective ROMPs and the properties of the tactic and the atactic hydrogenated ring-opened poly(DCPD)s. The three main purposes of the present study are as follows: first, to develop new tungsten(VI) imido and/or phenolate catalysts utilizable for stereoselective ROMP of DCPD; second, to elucidate the basic requirements for the regulation of the polymerization process using tungsten imido/phenolate catalysts; third, to investigate the thermal/mechanical properties of the crystalline isotactic and

\* Author for correspondence: e-mail tsunogae@zeon.co.jp.

syndiotactic hydrogenated poly(DCPD)s by various analytical methods.

## Experimental Section

**General Remarks.** All operations were carried out in a glovebox (nitrogen atmosphere,  $O_2 < 1$  ppm and  $H_2O < 1$  ppm) or under an argon atmosphere using standard Schlenk techniques.  $WCl_6$  (Soegawa Chemical),  $Et_2Al(OEt)$  (Kanto Chemical), and  $n-BuLi$  (Kanto Chemical) were used without further purification.  $WOCl_4$  was synthesized from  $WCl_6$  and hexamethyldisiloxane in methylene chloride.<sup>9</sup>  $WO(2,6-Me_2-phenolate)_4$  (**2**) and  $WO(racemic-5,5',6,6'-Me_4-3,3'-t-Bu_2-Biphenolate)_2$  ( $WO(rac-Biphenolate)_2$ ) (**3**) were prepared from  $WOCl_4$  and phenolates in diethyl ether as previously reported.<sup>8</sup> Grubbs catalyst,  $Ru(Cy_3P)_2Cl_2(=CHPh)$  (Aldrich), was used as received. Toluene, cyclohexane,  $n$ -pentane,  $n$ -hexane, and diethyl ether were distilled over sodium metal under an argon atmosphere before use. Methylene chloride was distilled over calcium hydride. Hexamethyldisiloxane was distilled over molecular sieves under reduced pressure. Phenyl isocyanate (Tokyo Kasei) was distilled from calcium hydride just prior to use. Commercially available  $(R)-(+)-5,5',6,6'$ -tertamethyl-3,3'-di-*tert*-butyl-1,1'-biphenyl-2,2'-diol ( $(R)-(+)-Biphenol$ ) (Strem), *racemic*-5,5',6,6'-tertamethyl-3,3'-di-*tert*-butyl-1,1'-biphenyl-2,2'-diol (*rac*-Biphenol) (Strem), and 2,6-dimethylphenol (Wako Chemicals) were used as received. *endo*-Dicyclopentadiene (DCPD) (Zeon Corp.) was distilled over calcium hydride under reduced pressure and stored as cyclohexane solution. 1-Octene (Wako Chemicals) was distilled over calcium hydride.

**$W(=NPh)Cl_4 \cdot Et_2O$  (**4**).** Freshly purified phenyl isocyanate (1.71 g, 14.4 mmol) was added to a suspension of  $WOCl_4$  (4.91 g, 14.4 mmol) in toluene (40 mL). The mixture was heated to reflux while it was stirred for 18 h to give a dark-green suspension. Dark-green microcrystals of the crude  $W(=NPh)Cl_4$  were collected from this suspension by centrifugation and then washed twice with a small amount of  $n$ -pentane. This material was dissolved in diethyl ether, and the green solution was filtered and dried in vacuo to yield the desired product as green microcrystals with 90% yield. Recrystallization from diethyl ether/ $n$ -hexane gave deep-green prism crystals of  $W(=NPh)Cl_4 \cdot Et_2O$  (**4**). Two crops of corresponding crystals were collected by filtration and dried in vacuo (yield 77% (5.46 g, 11.1 mmol)).  $^1H$  NMR ( $C_6D_6$ ):  $\delta$  6.97–6.87 (m, 4H,  $H_{aryl}$ ), 6.16 (t, 1H,  $H_{aryl}$ ), 4.43 (q, 4H,  $Et_2O$ ), 1.08 (t, 6H,  $Et_2O$ ).  $^{13}C$  NMR ( $C_6D_6$ ):  $\delta$  149.8, 134.0, 131.4, 127.2, 66.3, 13.1. Anal. Calcd for  $C_{10}H_{15}Cl_4$ -NOW: Calcd: C, 24.47; H, 3.08; N, 2.85. Found: C, 24.24; H, 3.00; N, 2.90.

**$W(=NPh)(2,6-Me_2-phenolate)_4$  (**5**).** Lithium 2,6-dimethylphenolate (4.97 g, 38.8 mmol) in diethyl ether (50 mL) was dropwise added to a diethyl ether solution (50 mL) of  $W(=NPh)Cl_4 \cdot Et_2O$  (4.76 g, 9.70 mmol) at  $-78^\circ C$ . The mixture was warmed to ambient temperature. The reaction mixture was stirred for 18 h to give a red solution. Diethyl ether was removed in vacuo, and the residue was extracted with toluene. The red extract was dried in vacuo to yield the desired product as a bright-red powder with 93% yield. Recrystallization was performed from  $n$ -hexane to give bright-red prism crystals of  $W(=NPh)(2,6-Me_2-phenolate)_4$  (**5**). The corresponding prism crystals were collected by filtration and dried in vacuo (yield 80% (5.92 g, 7.80 mmol)).  $^1H$  NMR ( $C_4D_8O$ ):  $\delta$  7.08 (t, 2H,  $H_{aryl}$ ), 6.83 (d, 8H,  $H_{aryl}$ ), 6.74 (t, 1H,  $H_{aryl}$ ), 6.57 (d, 4H,  $H_{aryl}$ ), 6.12 (d, 2H,  $H_{aryl}$ ), 2.01 (s, 24H,  $CH_3$ ).  $^{13}C$  NMR ( $C_4D_8O$ ):  $\delta$  162.5, 152.3, 128.7, 128.3, 127.3, 127.0, 126.8, 120.7, 17.2. Anal. Calcd for  $C_{38}H_{41}NO_4W$ : C, 60.09; H, 5.44; N, 1.84. Found: C, 61.03; H, 5.63; N, 1.89.

**$W(=NPh)((R)-(+)-5,5',6,6'-Me_4-3,3'-t-Bu_2-biphenolate)_2$  ( $W(=NPh)((R)-(+)-Biphenolate)_2$ ) (**6**).** Dilithium  $(R)-(+)-Biphenolate$  (4.19 g, 11.82 mmol) in diethyl ether (30 mL) was dropwise added to a diethyl ether solution (30 mL) of  $W(=NPh)Cl_4 \cdot Et_2O$  (2.90 g, 5.91 mmol) at  $-78^\circ C$ . The mixture was warmed to ambient temperature. The reaction mixture was stirred for 18 h to give a dark-red solution. Diethyl ether was removed in vacuo, and the residue was extracted with toluene. The dark-red extract was dried in vacuo to yield the desired product as a red powder with 96%

yield. Recrystallization from  $n$ -hexane gave red needle microcrystals of  $W(=NPh)((R)-(+)-Biphenolate)_2$  (**6**). Three crops of corresponding crystals were collected by filtration and dried in vacuo (yield 80% (4.63 g, 4.73 mmol)).  $^1H$  NMR ( $C_4D_8O$ ):  $\delta$  6.97 (s, 2H,  $H_{aryl}$ ), 6.91 (t, 2H,  $H_{aryl}$ ), 6.82 (s, 2H,  $H_{aryl}$ ), 6.55 (t, 1H,  $H_{aryl}$ ), 5.06 (d, 2H,  $H_{aryl}$ ), 2.28 (s, 6H,  $CH_3$ ), 2.16 (s, 6H,  $CH_3$ ), 1.59 (s, 6H,  $CH_3$ ), 1.54 (s, 6H,  $CH_3$ ), 1.42 (s, 18H, *t*-Bu), 1.20 (s, 18H, *t*-Bu).  $^{13}C$  NMR ( $C_4D_8O$ ):  $\delta$  161.9, 161.4, 151.1, 135.4, 133.4, 133.3, 132.8, 128.6, 128.4, 128.0, 127.5, 127.4, 126.2, 125.7, 125.5, 34.6, 34.2, 31.1, 30.9, 19.2, 19.1, 15.8, 15.3. Anal. Calcd for  $C_{54}H_{69}NO_4W$ : C, 66.18; H, 7.10; N, 1.43. Found: C, 65.87; H, 7.45; N, 1.65.

**Analyses of Complex and Polymer.**  $^1H$  and  $^{13}C$  NMR spectra were recorded on a JEOL JNM-EX400WB spectrometer (399.65 MHz for  $^1H$ , 100.40 MHz for  $^{13}C$ ), and chemical shifts were determined with reference to the residual benzene ( $\delta$  7.16 ppm for  $^1H$ , 128.0 ppm for  $^{13}C$ ), tetramethylsilane ( $\delta$  0.00 ppm), tetrahydrofuran ( $\delta$  3.53 ppm for  $^1H$ , 66.5 ppm for  $^{13}C$ ), *o*-dichlorobenzene ( $\delta$  127.5 ppm), or chloroform ( $\delta$  77.2 ppm). Elemental analyses were performed on a PE 2400 series II CHNS/O analyzer. The samples were sealed in tin foils under an argon atmosphere in a glovebox. The molecular weight distributions (MWD) of the polymers were obtained using a gel permeation chromatograph (GPC) (Tosoh HLC-8121 GPC/HT; eluent *o*-dichlorobenzene). The relative number- and weight-average molecular weights ( $M_n$  and  $M_w$ , respectively) were acquired by the use of a calibration curve obtained using polystyrene standards. Differential scanning calorimeter (DSC) measurements were performed on a Bruker AXS DSC3100SR in a dry nitrogen stream. Wide-angle X-ray diffraction (WAXD) of the polymers was recorded on Rigaku RINT 2500 diffractometer. Transmission electron microscopy (TEM) images were collected using a Hitachi H-7500 instrument. Films of tactic H-poly(DCPD)s were prepared by compression-molding just above their melting points. The isothermal crystallization was performed on the hot plate.

**Catalyst Preparation.** Polymerization catalyst solutions were prepared as follows unless otherwise stated: (i) A stirred toluene solution of  $W(=NPh)Cl_4 \cdot Et_2O$  (**4**) (0.0278 g, 56.7  $\mu$ mol) (green solution) was mixed with 3 equiv of  $Et_2Al(OEt)$  at room temperature. The mixture was aged for an additional 15 min and turned brown. (ii) To a toluene solution of  $W(=NPh)((R)-(+)-Biphenolate)_2$  (**6**) (0.0556 g, 56.7  $\mu$ mol) (dark-red solution) 2 equiv of  $n-BuLi$  was added at room temperature, and the mixture was stirred for 15 min to give a brown solution.

**Polymerization.** Polymerization was carried out at 50 or 80  $^\circ C$  in a prebaked ampule equipped with a rubber septum. A cyclohexane solution of DCPD (7.50 g, 56.7 mmol) and 1-octene (0.320 g, 2.83 mmol) was added to the catalyst mixture at the prescribed temperature. After stirring for a fixed time, the polymerization was quenched with a small amount of 2-propanol. The obtained polymer was reprecipitated from 2-propanol and was dried in vacuo at 40  $^\circ C$  for 24 h. The polymer yield was determined by gravimetric measurement.

**Hydrogenation.** A cyclohexane solution of poly(DCPD) and a cyclohexane solution of Ru-based hydrogenation catalyst were mixed in an autoclave under a dry nitrogen atmosphere. Then the dry nitrogen in the autoclave was replaced by dry hydrogen. The mixture was allowed to heat up to the hydrogenation temperature while stirring. Hydrogenation was carried out at 160  $^\circ C$  for 8 h under 1.0 MPa of  $H_2$ . After the hydrogenation reaction, the reaction mixture was cooled slowly to room temperature. In the course of this procedure, the crystallization of tactic H-poly(DCPD)s from the dilute solution occurred to form the highly crystalline tactic H-poly(DCPD)s as a fine powder. While atactic H-poly(DCPD) was amorphous, no crystallization from solution occurred. Ru-based hydrogenation catalyst solutions were prepared as follows:  $Ru-(Cy_3P)_2Cl_2(=CHOEt)$ , the precursor of hydrogenation catalyst, was prepared from  $Ru(Cy_3P)_2Cl_2(=CHPh)$  and 50-fold excess of ethyl vinyl ether.<sup>10</sup> According to the literature,  $RuCl_2(H_2)(PCy_3)_2$  or  $(PCy_3)_2ClRu(CO)(H)$  might be formed in the presence of  $H_2$  and possibly become an active species of hydrogenation.<sup>10</sup>

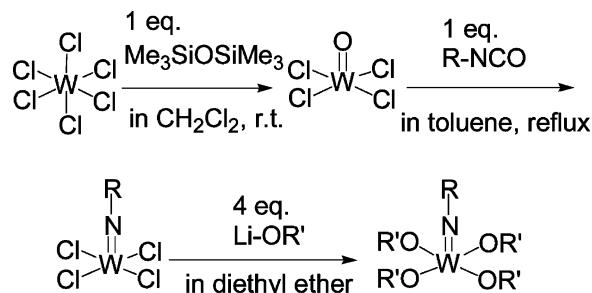
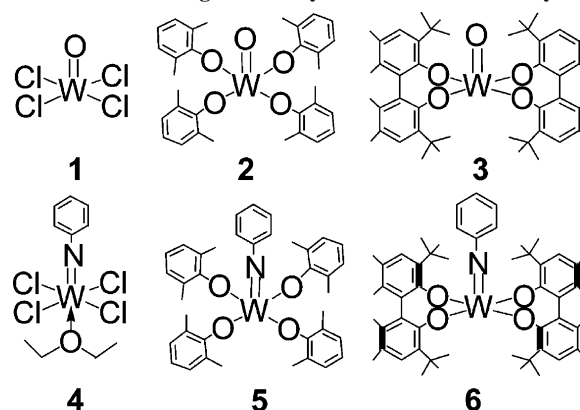
**Table 1.** Crystal Parameters of  $W(=NPh)(2,6-Me_2\text{-phenolate})_4$  (**5**)

parameter	
chem formula	$C_{38}H_{41}NO_4W$
FW	759.60
color	red
crystal system	triclinic
lattice params	
<i>a</i> , Å	10.970(3)
<i>b</i> , Å	16.109(3)
<i>c</i> , Å	21.208(6)
$\alpha$ , deg	106.53(2)
$\beta$ , deg	87.66(2)
$\gamma$ , deg	110.47(2)
<i>V</i> , Å <sup>3</sup>	3359(1)
space group	<i>P</i> -1
<i>Z</i>	4
<i>D</i> <sub>calc</sub> , g/cm <sup>3</sup>	1.500
$\mu$ (Mo K $\alpha$ ), cm <sup>-1</sup>	34.8
$2\theta_{max}$ , deg	60.1
oscillation range	
( $\phi = 0.0^\circ$ , $\chi = 45.0^\circ$ )	$\omega$ 130.0°–190.0° with 5.0° step
( $\phi = 180.0^\circ$ , $\chi = 45.0^\circ$ )	$\omega$ 0.0°–160.0° with 5.0° step
no. of reflections	total: 39717
	unique: 19076 ( <i>R</i> <sub>int</sub> = 0.054)
no. of observations	4454
no. of variables	875
goodness-of-fit on <i>F</i> <sup>2</sup>	1.00
<i>R</i> 1 ( <i>I</i> > 2.00 $\sigma$ )	0.026
<i>R</i> (all reflections) <sup>a</sup>	0.050
<i>wR</i> 2 (all reflections) <sup>b</sup>	0.066

**X-ray Structure Determination of 5.** A single crystal of **5** was mounted on a Rigaku RAXIS RAPID imaging plate for data collection using Mo K $\alpha$  radiation. Crystal data and data collection parameters of these complexes are summarized in Table 1. The data collections were performed at  $-180^\circ\text{C}$ . Indexing was performed for three oscillations, which were exposed for 60 s. The camera radius was 127.40 mm. Readout was performed in the 0.100 mm pixel mode. A numerical absorption collection was applied which resulted in transmission factors ranging from 0.39 to 0.50. The data were corrected for Lorentz and polarization effects. The structure of **5** was solved by heavy-atom Patterson methods (PATTY<sup>11</sup>) and expanded using Fourier techniques (DIRDIF99<sup>12</sup>). In the final refinement cycle of full-matrix least-squares refinement on *F*<sup>2</sup>, hydrogen atom locations were included at an idealized position, and the hydrogen atoms were given in the same temperature factor as that of carbon atoms to which they were bonded. All non-hydrogen atoms were anisotropically refined. All calculations were performed using the CrystalStructure crystallographic software package.

## Results and Discussion

**Catalyst Design and Synthesis of Tungsten(VI) Phenylimido Phenolate Complexes.** Thus far, isoselective ROMP has been achieved by several well-defined catalysts. Molybdenum alkylidene biphenolate complexes, so-called Schrock–Hoveyda catalysts, are known as effective initiators for isoselective ROMP of several cycloolefins. Previously, we have reported that the isoselective ROMP of DCPD occurs with oxomolybdenum (and oxotungsten) bisbiphenolate catalysts, such as  $MoO((R)-(+)-5,5',6,6'-Me_4-3,3'-t-Bu_2\text{-biphenolate})_2$ .<sup>8a,b,e</sup> Isoselectivity of the above-stated ROMP systems is supposed to originate from the enantiomeric site control caused by the bulky biphenolate ligand. Thus, the biphenolate ligand appears to be a key for isoselective regulation of the polymerization process. On the other hand, our recent study has verified that tungsten(VI) imido tetrachloride complexes such as  $W(=NPh)Cl_4 \cdot Et_2O$  were useful for the syndiospecific ROMP of DCPD.<sup>8c,d</sup> In the case of the W-arylimido-catalyzed polymerization, the syndioregularity decreased with increasing the steric size of substituents on the 2,6-position of the phenyl ring. For instance,

**Scheme 2.** Synthesis of Tungsten(VI) Imido Phenolate Complexes**Scheme 3.** Tungsten Catalysts in the Present Study

the poly(DCPD) obtained from  $W(=N-2,6-i-Pr_2Ph)Cl_4 \cdot Et_2O$  was atactic. Thus, non-ring-substituted phenylimido ligand appears suitable for realization of syndiospecific ROMP.

However, we have not yet done a thorough study of how the enchainment process would be regulated by the catalyst's ligands in the case of the above stereoselective ROMP catalysts. Again, the bulky biphenolate ligand is effective for the isoselective ROMP of DCPD, while the phenylimido ligand has some effect for the syndioregulation of ROMP. Therefore, it becomes interesting to investigate how the combination of phenylimido ligand and phenolate ligands regulates the polymerization process. These viewpoints led us to investigate the tungsten(VI) phenylimido Biphenolate catalysts.

As seen in Scheme 2,  $WCl_6$  was chosen as a starting material.  $WOCl_4$  was synthesized from  $WCl_6$  and hexamethyldisiloxane in methylene chloride according to the literature.<sup>9</sup> Then  $WOCl_4$  as catalyst precursor was treated with an equimolar of phenyl isocyanate under reflux conditions, and an analytically pure product of  $W(=NPh)Cl_4 \cdot Et_2O$  was obtained in moderate yield by recrystallization from diethyl ether.<sup>8c,d</sup> Then  $W(=NPh)Cl_4 \cdot Et_2O$  was mixed with 4 equiv of lithium 2,6-dimethylphenolate (or 2 equiv of dilithium (*R*)-(+)-Biphenolate) at  $-78^\circ\text{C}$ , and the mixture was allowed to react at ambient temperature. These products could be recrystallized from *n*-hexane to yield highly pure products.  $W(=NPh)(2,6-Me_2\text{-phenolate})_4$  (**5**) and  $W(=NPh)((R)-(+)\text{-Biphenolate})_2$  (**6**) were successfully synthesized. <sup>1</sup>H NMR, <sup>13</sup>C NMR, and elemental analysis identified these complexes. Additionally,  $WOCl_4$  (**1**),  $WO(2,6-Me_2\text{-phenolate})_2$  (**2**),  $WO(rac\text{-Biphenolate})_2$  (**3**), and  $W(=NPh)Cl_4 \cdot Et_2O$  (**4**) were synthesized<sup>8</sup> and used as polymerization catalysts for a comparison with the new catalysts (Scheme 3).

Single-crystal X-ray diffraction study on  $W(=NPh)(2,6-Me_2\text{-phenolate})_4$  (**5**) was carried out, and its molecular structure is depicted in Figure 1. Selected bond lengths and angles are also stated. The complex **5** has *C*<sub>1</sub> symmetric distorted square-pyramidal geometry with the phenylimido ligand in the apical



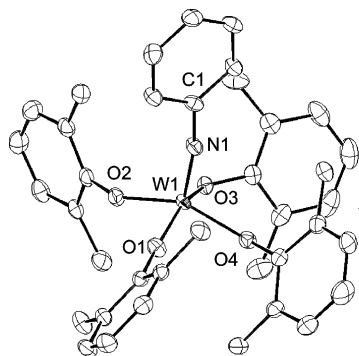


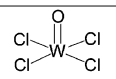
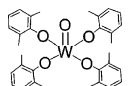
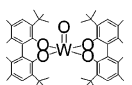
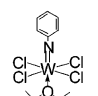
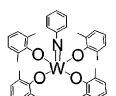
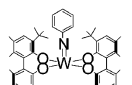
**Figure 1.** ORTEP representation of  $W(=NPh)(2,6\text{-Me}_2\text{-phenolate})_4$  (**5**) with 50% probability thermal ellipsoids. Selected bond angles and distances: angles (deg),  $W(1)\text{--}N(1)\text{--}C(1) = 169.0(2)$ ,  $N(1)\text{--}W(1)\text{--}O(1) = 103.26(11)$ ,  $N(1)\text{--}W(1)\text{--}O(3) = 105.17(11)$ ; distances (Å),  $W(1)\text{--}N(1) = 1.732(2)$ ,  $N(1)\text{--}C(1) = 1.402(3)$ ,  $W(1)\text{--}O(1) = 1.863(2)$ ,  $W(1)\text{--}O(3) = 1.933(2)$ .

position. The  $W(1)\text{--}N(1)$  bond length ( $1.732(2)$  Å) and  $W(1)\text{--}N(1)\text{--}C(1)$  angle ( $169.0(2)^\circ$ ) indicate the strong donation of the nitrogen lone pair and sp hybridization about the N atom. The relatively short  $N(1)\text{--}C(1)$  distance ( $1.402(3)$  Å) also supports the conjugation system of the nitrogen atom from phenyl ring. These bond lengths and angle are comparable to those of the previously reported **4**:  $W\text{--}N$  ( $1.727(4)$  Å);  $N\text{--}C$  ( $1.378(6)$  Å);  $W\text{--}N\text{--}C$  ( $176.4(2)^\circ$ ).<sup>8d</sup> The  $W(1)\text{--}N(1)\text{--}C(1)$  angle of complex **5** is narrower than that of **4**, indicating that the electron donation of the nitrogen lone pair of **5** is weaker than that of **4**. Each of  $N\text{--}W\text{--}O$  angles of **5** is found to be different, probably owing to the steric/electronic effect arising from phenylimido ligand. In contrast, previously reported  $MoO\text{--}$

$(2,6\text{-Me}_2\text{-phenolate})_4$  was a  $C_4$  symmetric and square-pyramidal structure, and the  $O1\text{--}Mo\text{--}O2$  angle is  $104.75(7)^\circ$  and similar to the average of each  $N\text{--}W\text{--}O$  angles ( $105.49(12)^\circ$ ).<sup>8d</sup> The distance of the W and oxygen atom of the phenolate ( $1.909(2)$  Å) in **5** is also close to that of the Mo and oxygen atom of phenolate ligand ( $1.881(2)$  Å) of the  $MoO(2,6\text{-Me}_2\text{-phenolate})_4$ .

**Stereocontrol by Imido and/or Phenolate Ligands: Stereoselective Polymerization of DCPD with Various Tungsten Catalysts.** Table 2 summarizes the results of the optimized DCPD polymerizations using several tungsten imido and/or phenolate catalysts and of the successive hydrogenations of the obtained poly(DCPD)s. At first, we performed all the polymerizations without chain transfer agent. However, the polymerization mixtures became a very viscous gel, and the molecular weights of the obtained poly(DCPD)s were hard to determine by GPC, probably due to their high molecular weights. The molecular weights of the poly(DCPD)s should be controlled in the suitable range ( $M_n$ :  $10^3\text{--}10^5$ ) for the further analytical study. Therefore, we decided to add an adequate amount of 1-octene as a chain transfer reagent in all the polymerization systems. The **1**–**6** induced the polymerization of DCPD smoothly to provide poly(DCPD)s in high yields. The poly(DCPD)s obtained from **1**, **4**, and **5** were highly soluble in ordinary organic solvents, while poly(DCPD) yielded by **2** was less soluble, probably due to its high molecular weight.<sup>14</sup> Those produced by **3** and **6** were insoluble at room temperature, probably because those polymers were isotactic (vide infra). Thus, the poly(DCPD)s were characterized by a combination of  $^1H$  NMR and GPC at high temperature ( $150^\circ C$ ) because all the poly(DCPD)s were soluble in *o*-dichlorobenzene at  $150^\circ C$ . It was found that the molecular weights of all the poly(DCPD)s were kept in the

**Table 2.** Polymerization of DCPD by Various Tungsten Catalysts and Sequential Hydrogenation of the Obtained Ring-Opened Poly(DCPD)s

catalysts	poly(DCPD)s				hydrogenated poly(DCPD)s <sup>c</sup>		
	<i>M</i> <sub>n</sub>	<i>M</i> <sub>w</sub> / <i>M</i> <sub>n</sub>	cis/trans	thermal properties <sup>d</sup>	meso/racemo	thermal properties <sup>d</sup>	
	<b>1<sup>a</sup></b>	10 500	2.5	77/23	T <sub>g</sub> = 140 °C	50/50	T <sub>g</sub> = 101 °C
	<b>2<sup>b</sup></b>	not determined <sup>e</sup>		60/40	T <sub>g</sub> = 131 °C	55/45 <sup>f</sup>	T <sub>g</sub> = 106 °C
	<b>3<sup>b</sup></b>	7 800	3.1	91/9	T <sub>m</sub> = 264 °C 29 J/g	95/5	T <sub>m</sub> = 292 °C 44 J/g
	<b>4<sup>a</sup></b>	8 200	3.4	93/7	T <sub>g</sub> = 151 °C	20/80	T <sub>m</sub> = 272 °C 52 J/g
	<b>5<sup>b</sup></b>	50 000	2.6	72/28	T <sub>g</sub> = 147 °C	43/57	T <sub>g</sub> = 102 °C
	<b>6<sup>b</sup></b>	8 000	2.8	97/3	T <sub>m</sub> = 260 °C 21 J/g	95/5	T <sub>m</sub> = 291 °C 41 J/g

<sup>a</sup> Polymerized in cyclohexane at rt for 24 h; [DCPD] = 20 wt % (1.3 M), [1-octene] = 50 mM, [W complex] = 1.3 mM, [W complex]:[Et<sub>2</sub>Al(OEt)] = 1:3, all polymer yields were 100%. <sup>b</sup> Polymerized in cyclohexane at  $80^\circ C$  for 3 h; [DCPD] = 20 wt % (1.3 M), [1-octene] = 50 mM, [W complex] = 1.3 mM, [W complex]:[*n*-BuLi] = 1:2, all polymer yields were 100%. <sup>c</sup> Hydrogenated in cyclohexane at  $160^\circ C$  for 8 h; [Ru(Cy<sub>3</sub>P)<sub>2</sub>Cl<sub>2</sub>(=CHOEt)]/[DCPD unit] = 1/1000 in mole ratio, [poly(DCPD)] = 5 wt %,  $H_2 = 1.0$  MPa, all polymers' hydrogenation ratios were 100%. <sup>d</sup> First scan of the DSC measurement. <sup>e</sup> See ref 14. <sup>f</sup> Hydrogenation reaction has leveled off at hydrogenation ratio 98%.

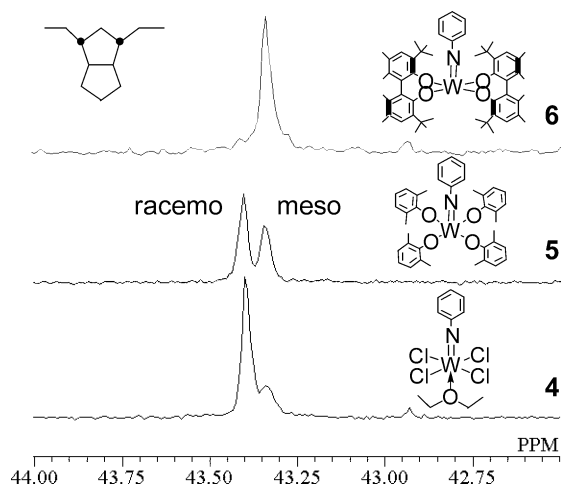


**Figure 2.**  $^{13}\text{C}$  NMR spectra of methyne carbons in the main chain of H-poly(DCPD)s shown in Table 2.

range of 7000–50 000, except for that of **2**. The solubility and the  $^1\text{H}$  NMR spectra suggested that all the present poly(DCPD)s were linear and non-cross-linked polymers through selective ring-opening of strained norbornene ring and retained the less-strained cyclopentene ring. Further, we have conducted the polymerization of 3,4-dihydro-DCPD by catalysts **1–6**, but no vinyl addition-type oligomer was obtained. This result also supported the complete linearity of the present ring-opened poly(DCPD)s.

The stereoregularity of the polymerization was determined by  $^{13}\text{C}$  NMR measurements on the hydrogenated ring-opened poly(DCPD)s (H-poly(DCPD)s) at 150  $^\circ\text{C}$ , and the signals for the methyne carbons are shown in Figure 2. The *cis*-regularity was also estimated by  $^{13}\text{C}$  NMR spectra of the ring-opened poly(DCPD)s.<sup>5a</sup> As seen in Table 2,  $\text{WOCl}_4$  polymerized DCPD to produce *cis*-rich and atactic polymer. The tungsten oxo phenolate complex,  $\text{WO}(\text{2,6-Me}_2\text{-phenolate})_4$  (**2**), also afforded *cis*-rich and atactic polymer. This result suggested that the 2,6- $\text{Me}_2$ -phenolate ligand is less effective for tacticity control of the ROMP process. As reported,  $\text{WO}(\text{rac-Biphenolate})_2$  (**3**) was a useful catalyst for the *cis*-, isoselective ROMP of DCPD. Hence, the biphenolate ligand proved to be effective for isoselective ROMP. Then the effect of the tungsten imido phenolate complexes were examined on the polymerization,  $\text{W}(=\text{NPh})\text{Cl}_4 \cdot \text{Et}_2\text{O}$  (**4**) promoted the *cis*-, syndioselective ROMP of DCPD, and the tungsten imido phenolate catalyst,  $\text{W}(=\text{NPh})(\text{2,6-Me}_2\text{-phenolate})_4$  (**5**), gave a slightly syndio-biased polymer. It is interesting that  $\text{W}(=\text{NPh})((\text{R})-(+)\text{-Biphenolate})_2$  (**6**) exhibited a notable ability to regulate the polymerization process: high-*cis* and isotactic poly(DCPD) was obtained using **6** as initiator.

It can be said that the stereoregularity of the present polymerization systems was highly dependent on the catalyst design. To compare the result of polymerization initiated by **1** and by **4**, one can say that the terminal oxo ligand was ineffective to govern the polymerization process, whereas the phenylimido ligand could lead the enchainment reaction into a syndioregular manner. However, the stereocontrolling ability of the phenylimido ligand was likely to be very limiting. Comparing **5** with **4**, the introduction of 2,6- $\text{Me}_2$ -phenolate ligand on **4** appeared to cancel the stereoregulation effect of phenylimido ligand. Moreover, the effect of bulky biphenolate probably overwhelmed the effect of phenylimido ligand to lead the polymerization into isoselective. It appears that the influence of the phenolate ligand on the polymerization process can be compared favorably with that of the phenylimido ligand. These tendencies are very similar to those observed in stereospecific polymerizations using Schrock catalysts and Schrock–Hoveyda catalysts.<sup>4</sup>

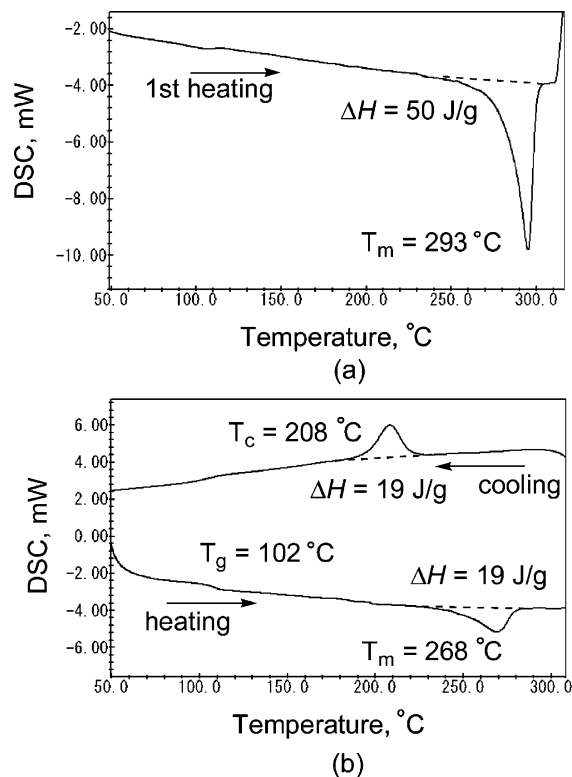


**Figure 3.** DSC thermograms of the iso-H-poly(DCPD) produced by **3** described in Table 2 (determined on the first heating scan for (a) and on the second scan for (b) under  $\text{N}_2$  for 10  $^\circ\text{C}/\text{min}$ ).

The thermal properties of the present ring-opened poly(DCPD)s were characterized by DSC. The poly(DCPD)s, which were produced by **1**, **2**, **4**, and **5**, shown only glass transitions in the range of 130–160  $^\circ\text{C}$ . This suggests that the *cis*-syndiotactic poly(DCPD) and the atactic poly(DCPD)s were amorphous polymers. By contrast, the insoluble poly(DCPD)s, whose main chains were high-*cis* and isotactic, proved to be crystalline. Those insoluble poly(DCPD)s exhibited first-order transitions at high temperatures. DSC measurements of the corresponding hydrogenated ring-opened poly(DCPD)s were also conducted. As expected, atactic H-poly(DCPD)s, which were produced by **1**, **2**, and **5**, possessed only glass transitions and no crystalline melting behavior. This result suggests that atactic H-poly(DCPD)s were amorphous polymers. Crystalline syndiotactic H-poly(DCPD) was obtained from  $\text{W}(=\text{NPh})\text{Cl}_4 \cdot \text{Et}_2\text{O}$  (**4**). Within the experimental limits, the thermal properties of the samples of crystalline isotactic H-poly(DCPD)s yielded by **3** and **6** were identical. This result also supports the view that the effect of the biphenolate ligand is larger than that of phenylimido ligand.

**Characterization and Properties of the Isotactic- (and the Syndiotactic-) Hydrogenated Poly(DCPD)s.** Properties of tactic hydrogenated ring-opened poly(DCPD)s and that of atactic counterpart, which are described in Table 2, were investigated in detail (isotactic-H-poly(DCPD) (iso-H-poly(DCPD)) prepared by **3**, syndiotactic-H-poly(DCPD) (syndio-H-poly(DCPD)) by **4**, and atactic-H-poly(DCPD) (ata-H-poly(DCPD)) by **5**). It is worth noting that the iso- and syndio-H-poly(DCPD)s were proven to be crystalline polymers.

Under DSC analysis during both the first heating and the second heating of the iso-H-poly(DCPD), first-order transitions were exhibited at elevated temperatures (Figure 3). This result clearly suggests that the iso-H-poly(DCPD) is a crystalline polymer. In addition to the melting point, the glass transition point was also observed at 102  $^\circ\text{C}$  on the second heating trace.

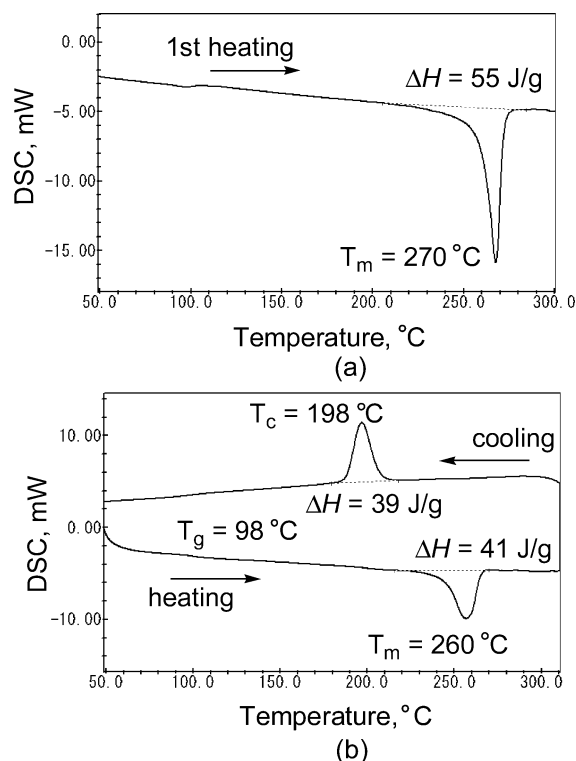


**Figure 4.** DSC thermograms of the syndio-H-poly(DCPD) with **4** described in Table 2 (determined on the first heating scan for (a) and on the second scan for (b) under N<sub>2</sub> for 10 °C/min).

As seen in Figure 4, the DSC traces of both the first heating and the second heating of the syndio-H-poly(DCPD) also showed large endothermic peaks at high temperatures, suggesting a highly crystalline material (Figure 4). This polymer also showed the glass transition at 98 °C on the second scan. From these results, it is presumed that the thermal property of the syndio-H-poly(DCPD) was comparable with that of the iso-H-poly(DCPD). In both polymers, the melting enthalpy of first scan was larger than that of the second scan. This can be explained by the idea that the hydrogenated tactic poly(DCPD)s without heat hysteresis is different from the melted and cooled bulk polymers. In general, crystallization of polymer from dilute solution attains a high crystallinity, while the crystallization of the polymer melt generally gives a lower crystallinity. One difference, however, was observed between two polymers: on the second heating, the isotactic polymer displayed relatively small melting enthalpy about 20 J/g, whereas syndiotactic polymer possessed large melting enthalpy ( $\Delta H = 40$  J/g). The WAXD measurements indicate that the crystal size/structure of both polymers are dissimilar (vide infra). In contrast, the atactic H-poly(DCPD) exhibited only a glass transition at 101 °C and no crystal melting (Figure 5). It is interesting to note that the tactic H-poly(DCPD)s are crystalline polymers, whereas the atactic polymer is amorphous. In contrast to the H-poly(DCPD)s, both the atactic and "tactic" hydrogenated ring-opened polynorbornenes are crystalline.<sup>7,8b</sup> To conclude this paragraph, it can be said that the stereostructure of the backbone significantly affects the higher order structure of the H-poly(DCPD).

Further, the crystalline nature of the tactic H-poly(DCPD)s was investigated by a combination of transmission electron microscopy (TEM) and wide-angle X-ray diffraction (WAXD). Quench-cooled films and fully annealed films of both the tactic H-poly(DCPD)s were prepared by heat compression molding. At first, powder of polymer was compressed and melted just above its melting point. Then the polymer melt was quench-

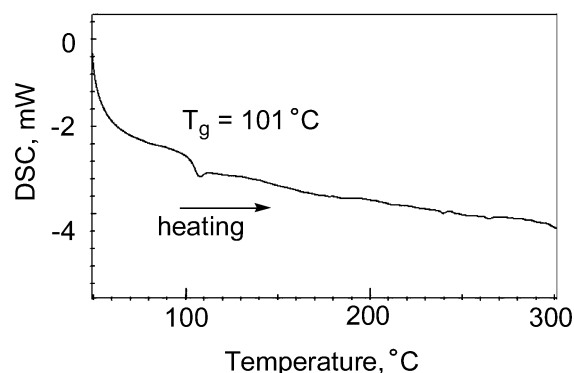


**Figure 5.** DSC thermograms of the atactic H-poly(DCPD) with **5** described in Table 2 (determined on the second scan under N<sub>2</sub> for 10 °C/min).

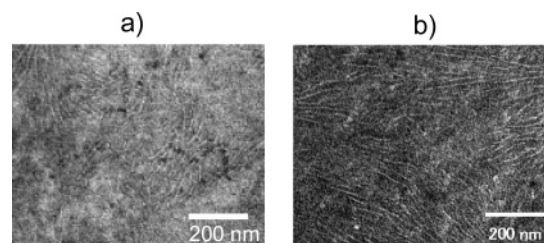


**Figure 6.** TEM images of the fully annealed and ultrathin-sectioned specimens of (a) the iso-H-poly(DCPD) produced by **3** and of (b) the syndio-H-poly(DCPD) produced by **4** represented in Table 2.

cooled by liquid N<sub>2</sub> to give amorphous tactic polymer film. The annealing of the polymer films was conducted at 180 °C for 1 h. The quench-cooled polymer films were entirely transparent. It is interesting to note that the fully annealed polymer films of about 0.1 mm thickness were almost transparent. This indicated that the crystal size of both the tactic H-poly(DCPD)s might be very small.

The TEM morphologies of RuO<sub>4</sub>-stained and ultrathin-sectioned specimens strongly implied that both the fully annealed iso- and syndio-H-poly(DCPD)s were crystalline polymers (Figure 6). It could be emphasized that no spherulite was observed in either tactic polymers. This result is consistent with the high transparency of both the fully annealed polymer film (vide supra). Only the lamellar crystals of about 6–8 nm of thickness appeared to have grown without any orientation during the course of isothermal crystallization.

A WAXD study of the iso- and the syndio-H-poly(DCPD)s was conducted next. Figure 7 shows diffraction patterns for (a) the iso- and (b) the syndio-H-poly(DCPD)s, following three very different thermal hysteresis described in the caption (Figure 7). The WAXD patterns of (i) the fine powders without heat history of both tactic polymers exhibited sharp crystalline peaks. Similarly, the fully annealed films of each polymer also showed crystalline peaks, while the diffraction patterns of the quench-cooled films only possessed amorphous halo. As expected, the diffraction patterns of the syndio-H-poly(DCPD) were entirely different from that of the iso-H-poly(DCPD). This result suggests that the crystal structures of the H-poly(DCPD)s are dependent on the stereostructure of their polymer backbones. The weight fraction crystallinity ( $w_c$ ) of the fully annealed iso-H-poly(DCPD) was evaluated by separation of crystalline peaks and amorphous halo, yielding  $w_c = 0.24$ . Similarly, the  $w_c$  of the fully annealed syndio-H-poly(DCPD) was 0.21, whereas the  $w_c$  of the syndio-H-poly(DCPD) obtained from solution and free of heat hysteresis was estimated to be 0.61 and remarkably high. Likewise,  $w_c$  of the iso-H-poly(DCPD) without heat history was

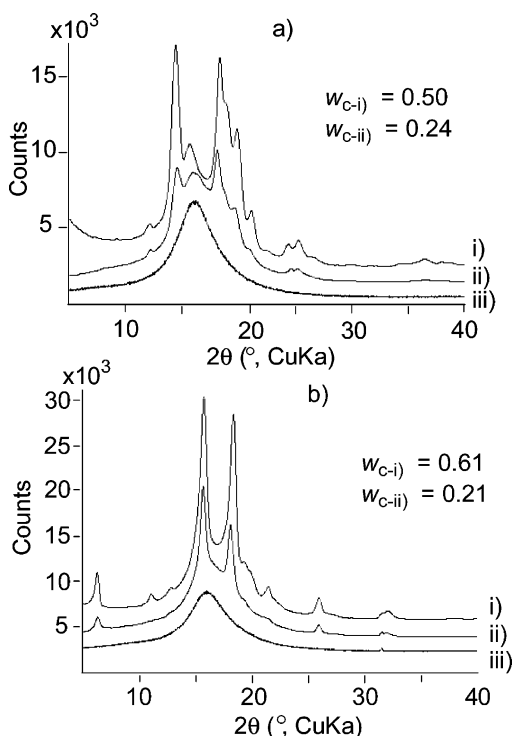
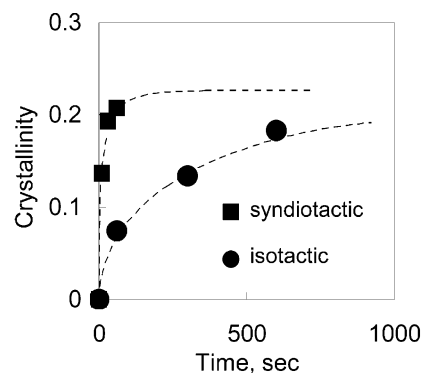


**Figure 7.** WAXD patterns of (i) the powder without heat hysteresis, (ii) the fully annealed film, and (iii) the quench-cooled film of (a) the iso-H-poly(DCPD) by **3** and (b) the syndio-H-poly(DCPD) by **4**. (The  $w_c$  of the iso-H-poly(DCPD) without heat hysteresis; 0.50, the  $w_c$  of the fully annealed iso-H-poly(DCPD); 0.24, the  $w_c$  of the syndio-H-poly(DCPD) without heat hysteresis; 0.61, the  $w_c$  of the fully annealed syndio-H-poly(DCPD); 0.21.)

0.50 and also high. From these results, it can be concluded that both tactic H-poly(DCPD)s can be regarded as highly crystalline polymers.

Moreover, the crystallization kinetics of both tactic polymers were studied. The films of syndio- and iso-H-poly(DCPD)s were prepared by compression molding just above their melting points. The isothermal crystallization was performed on a hot plate, and the crystallinity was estimated by WAXD. The saturated crystallinity ( $X_s$ ) of the syndio- and the iso-H-poly(DCPD)s were found to be 0.21 and 0.24, respectively, and constant in the range of 170–210 °C. Thus, we decided to conduct the isothermal crystallization experiments of both polymers at 180 °C with the motivation to compare the crystallization rate of both tactic polymers at the same temperature. The kinetic parameters of isothermal crystallizations were determined by the double-logarithmic plot of the following modified Avrami equation:  $\ln(1 - X(t)/X_s) = -k_c t^n$ , where  $X(t)$  is the relative crystallinity at crystallization time  $t$ ,  $X_s$  is the saturated crystallinity,  $k_c$  is the crystallization rate constant, and  $n$  is the Avrami exponent.

It is important to note that the syndio-H-poly(DCPD) was found to be characterized by a high crystallization rate (Figure 8). As seen in Figure 8, the  $k_c$  of the syndio-H-poly(DCPD) was verified to be 5 times higher than that of the isotactic counterpart. Short crystallization half-time also supported the significant improvement in the crystallization rate. The unique value of the Avrami exponents indicated the complicated mechanism of the phase transition of the both tactic H-poly(DCPD)s. The low values of the Avrami exponents of the syndio-H-poly(DCPD) and of the iso-H-poly(DCPD) indicated one- or two-dimensional crystal growth, which would produce fibril or lamellar crystals. This inference is consistent with the crystal form information given by the TEM morphology (vide



tacticity	crystallization rate constant, $k_c$	Avrami exponent, $n$	crystallization half-time, $t_{1/2}$
isotactic	$0.035 \text{ s}^{-1}$	0.57	188
syndiotactic	$0.171 \text{ s}^{-1}$	0.79	5.9

**Figure 8.** Crystallization kinetics of the iso-H-poly(DCPD) by **3** and the syndio-H-poly(DCPD) by **4** (isothermal crystallization was performed at 180 °C; the crystallinity was estimated by WAXD; the kinetic parameters of isothermal crystallizations were determined by the double-logarithmic plot of the following modified Avrami equation:  $\ln(1 - X(t)/X_s) = -k_c t^n$ , where  $X(t)$  is the relative crystallinity at crystallization time  $t$ ,  $X_s$  is the saturated crystallinity,  $k_c$  is the crystallization rate constant, and  $n$  is the Avrami exponent).

supra). It is plausible that the nucleation of both polymers was heterogeneous, consistent with the low values of the Avrami coefficients. It can be presumed that the crystal growth of the iso-H-poly(DCPD) was diffusion-controlled and one-dimensional process. On the other hand, the Avrami exponent of the syndio-H-poly(DCPD) gave no clear suggestion on the nature of crystal growth. At least it is assumable that the phase transition of the syndio-H-poly(DCPD) was dominated by the combination of such factors as the low and intermediate dimensionality of crystal growth and/or mixed crystal growth of interface- and diffusion-controlled mechanisms. It is presumed that the rigid ring structure of the main chain might hold a key role in the crystal growth of the both tactic H-poly(DCPD)s, and the detailed investigation is now in progress.

## Summary

In this paper, we have studied various iso- and syndioselective ROMP catalysts and the properties of the tactic and atactic hydrogenated ring-opened poly(DCPD)s. First, we have uncovered the basic requirements for the stereoregulation of the polymerization process using tungsten imido/phenolate catalysts. The phenylimido ligand seems to play an important role in achieving *cis*-, syndioselective ROMP, while bulky biphenolate ligands overwhelm the effects of imido ligand to lead the polymerization into *cis*-, isoselective. To the best of our knowledge, the series of tungsten(VI) oxo/phenolate and imido/phenolate complexes of the present study appear to be very versatile catalysts for stereoselective ROMPs from the point of view of the practical application. We suppose that the syntheses and preparations of these binary catalysts are simple and easy as compared to those of the well-defined metal carbene complexes. Second, we have shown that the tactic hydrogenated poly(DCPD)s were characterized by their high thermal stability. These polymers were revealed to be crystalline polymers. No spherulite and only lamellar crystals were observed in both tactic polymers. Particularly, practical application of the syndiotactic hydrogenated poly(DCPD) might be promising due to its high crystallization rate. We hope that the present study may broaden



the utility of the stereoselective ROMP and of the hydrogenated poly(cyclic olefin)s.

**Acknowledgment.** The authors thank Prof. Takeshi Shiono, Prof. Yuushou Nakayama, Dr. Hideaki Iwatani, Dr. Mikio Yamasaki, Dr. Motoo Shiro, and Ms. Jean Aizawa for their helpful discussions.

**Supporting Information Available:** Experimental details, final positional parameters, final thermal parameters, and bond distances and angles for **5**. This material is available free of charge via the Internet at <http://pubs.acs.org>.

## References and Notes

- (1) For a recent book: (a) Grubbs, R. H. *Handbook of Metathesis*; Wiley-VCH: Weinheim, 2003. (b) Ivin, K. J.; Mol, J. C. *Olefin Metathesis and Metathesis Polymerization*; Academic Press: San Diego, 1997.
- (2) For a recent review: (a) Schrock, R. R. *Handbook of Metathesis*; Grubbs, R. H., Ed.; Wiley-VCH: Weinheim, 2003; Vol. 1, pp 8–32 and references therein. (b) Schrock, R. R.; Hoveyda, A. H. *Angew. Chem., Int. Ed.* **2003**, *42*, 4592. (c) Schrock, R. R. *Chem. Rev.* **2002**, *102*, 145. (d) Hoveyda, A. H.; Schrock, R. R. *Chem.—Eur. J.* **2001**, *7*, 945. (e) Buchmeiser, M. R. *Chem. Rev.* **2000**, *100*, 1565.
- (3) (a) Nguyen, S. T.; Trnka, T. M. In *Handbook of Metathesis*, Grubbs, R. H., Ed.; Wiley-VCH: Weinheim, 2003; Vol. 1, pp 61–85 and references therein. (b) Sanford, M. S.; Love, J. A. In *Handbook of Metathesis*, Grubbs, R. H., Ed.; Wiley-VCH: Weinheim, 2003; Vol. 1, pp 112–131 and references therein. (c) Black, G.; Maher, D.; Risse, W. In *Handbook of Metathesis*; Grubbs, R. H., Ed.; Wiley-VCH: Weinheim, 2003; Vol. 3, pp 2–71 and references therein.
- (4) Hamilton, J. G. In *Handbook of Metathesis*, Grubbs, R. H., Ed.; Wiley-VCH: Weinheim, Vol. 3, pp 143–179 and references therein.
- (5) (a) Hamilton, J. G.; Ivin, K. J.; Rooney, J. J. *J. Mol. Catal.* **1986**, *36*, 115. (b) Al-Samak, B.; Ebrahimi, V. A.; Carvill, A. G.; Hamilton, J. G.; Rooney, J. J. *Polym. Int.* **1996**, *41*, 85. (c) Carvill, A. G.; Greene, R. M. E.; Hamilton, J. G.; Ivin, K. J.; Kenwright, A. M.; Rooney, J. J. *Macromol. Chem. Phys.* **1998**, *199*, 687.
- (6) Yamazaki, M. *J. Mol. Catal. A: Chem.* **2004**, *213*, 81.
- (7) (a) Lee, L. W.; Register, R. A. *Macromolecules* **2004**, *37*, 7278. (b) Lee, L. W.; Register, R. A. *Macromolecules* **2005**, *38*, 1216.
- (8) (a) Hayano, S.; Kurakata, H.; Uchida, D.; Sakamoto, M.; Kishi, N.; Matsumoto, H.; Tsunogae, Y.; Igarashi, I. *Chem. Lett.* **2003**, *32*, 670. (b) Hayano, S.; Kurakata, H.; Tsunogae, Y.; Nakayama, Y.; Sato, Y.; Yasuda, H. *Macromolecules* **2003**, *36*, 7422. (c) Hayano, S.; Tsunogae, Y. *Chem. Lett.* **2005**, *34*, 1520. (d) Hayano, S.; Tsunogae, Y. *Macromolecules* **2006**, *39*, 30. (e) Hayano, S.; Sugawara, T.; Tsunogae, Y. *J. Polym. Sci., Part A: Polym. Chem.* **2006**, *44*, 3153.
- (9) Gibson, V. C.; Kee, T. P.; Shaw, A. *Polyhedron* **1988**, *7*, 579.
- (10) (a) Drouin, S. D.; Yap, G. P. A.; Fogg, D. E. *Inorg. Chem.* **2000**, *39*, 5412. (b) Louie, J.; Grubbs, R. H. *Organometallics* **2002**, *21*, 2153.
- (11) Beurskens, P. T.; Admiraal, G.; Beurskens, G.; Bosman, W. P.; Garcia-Granda, S.; Gould, R. O.; Smits, J. M. M.; Smykalla, C. The DIRDIF program system, Technical Report of the Crystallography Laboratory, University of Nijmegen, The Netherlands, 1992.
- (12) Beurskens, P. T.; Admiraal, G.; Beurskens, G.; Bosman, W. P.; de Gelder, R.; Israel, R.; Smits, J. M. M. The DIRDIF-99 program system, Technical Report of the Crystallography Laboratory, University of Nijmegen, The Netherlands, 1999.
- (13) Pederson, S. F.; Schrock, R. R. *J. Am. Chem. Soc.* **1982**, *104*, 7483.
- (14) The molecular weight was hard to determine accurately by GPC, because the MW was extremely high. Beyond our presumption, **2** produced high molecular weight polymer even when 1-octene itself was employed as a polymerization solvent. Therefore, it can be concluded that the **2**-based catalyst was less reactive to terminal olefins, which were employed as a chain-transfer agent in the present polymerization systems.

MA0604340